Electronic Supplementary Information

In-situ synthesis of magnesium hydroxides modified with tripodal ligands in an organic medium

Keisuke Muramatsu,[a] Yoshiyuki Kuroda,*[b, #] Atsushi Shimojima,[c] Hiroaki Wada[c] and Kazuyuki Kuroda*[c, d]

a Department of Advanced Science and Engineering, Faculty of Science and Engineering, Waseda University, 3-4-1 Ohkubo, Shinjuku-ku, Tokyo, 169-8555, Japan.

b Waseda Institute for Advanced Study, Waseda University, 1-6-1 Nishiwaseda, Shinjuku-ku, Tokyo 169-8050, Japan.

c Department of Applied Chemistry, Faculty of Science and Engineering, Waseda University, 3-4-1 Ohkubo, Shinjuku-ku, Tokyo, 169-8555, Japan.

d Kagami Memorial Research Institute for Materials Science and Technology, Waseda University, 2-8-26 Nishiwaseda, Shinjuku-ku, Tokyo, 169-0051, Japan.

Present address: Green Hydrogen Research Center, Yokohama National University, 79-5 Tokiwadai, Hodogaya-ku, Yokohama, 240-8501, Japan.

Contents

The reason for the selection of DMSO as a solvent.

Because the solvent is required to dissolve both $MgCl_2·6H_2O$ and Tris-NH_2 for the synthesis of Mg-Tris-NH_2, the solubilities of $MgCl_2·6H_2O$ and Tris-NH_2 in several organic solvents (i.e., dimethyl sulfoxide (DMSO), *N*,*N*-dimethylformamide (DMF), and *N*,*N*-dimethylacetamide (DMA)) were examined. While each solvent dissolved sufficient amounts of $MgCl_2·6H_2O$, the solubilities of Tris-NH_2 in these solvents were significantly different. DMSO completely dissolves Tris-NH_2 with a concentration of 1.0 M at room temperature, whereas the saturated concentrations of Tris-NH_2 in DMF and DMA were approximately 0.2 M even under heating. On the basis of these results, we chose DMSO as an optimum solvent for the synthesis of Mg-Tris-NH_2.

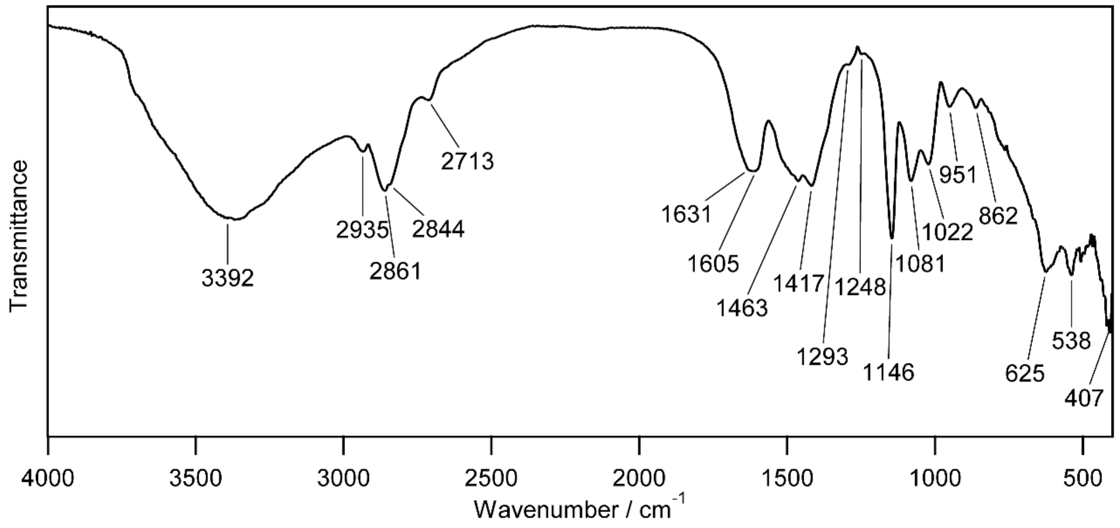

Fig. S1 FTIR spectrum of Mg-Tris-NH$_2$(98).

Table S1 Assignments of the infrared absorption bands of Mg-Tris-NH$_2$(98).[1]

Wavenumber /cm^{-1}	Vibration
407	Mg–O lattice vibration
538	Mg–O lattice vibration
625	τCO
862	δHCC
951	δHCC
1022	υCO
1081	υCO
1146	υCC
1248	υCC
1417	υCO (CO_3^{2-})
1463	δCH$_2$
1600–1630	δHNH and δH$_2$O
2713	Unknown, possibly arising from combinations and/or overtone.
2844	υ_{sym}CH
2861	υ_{sym}CH (possibly due to the hydroxyl methyl groups which are not bonded with the brucite layer)
2935	υ_{asym}CH
3392 (broad)	υOH (surface hydroxy groups and H$_2$O) and υNH

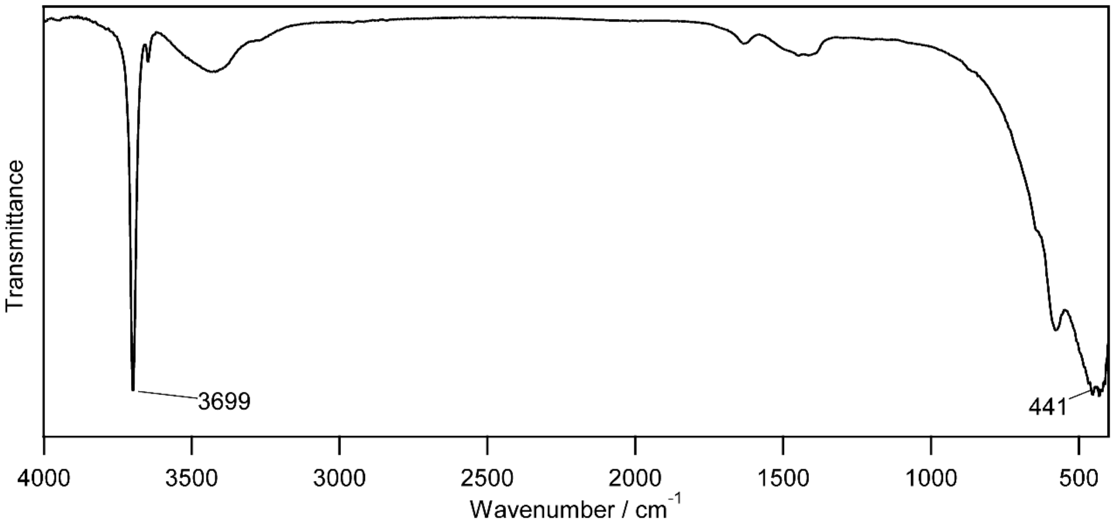

Fig. S2 FTIR spectrum of $Mg(OH)_2$ in the range of 400–4000 cm^{-1}. Sharp absorption band at 3699 cm^{-1} is due to free hydroxy groups. The Mg–O lattice vibrational band is observed at around 441 cm^{-1}. In the far-infrared region (not shown), another absorption band due to Mg–O lattice vibration should appear at around 368 cm^{-1}.[2]

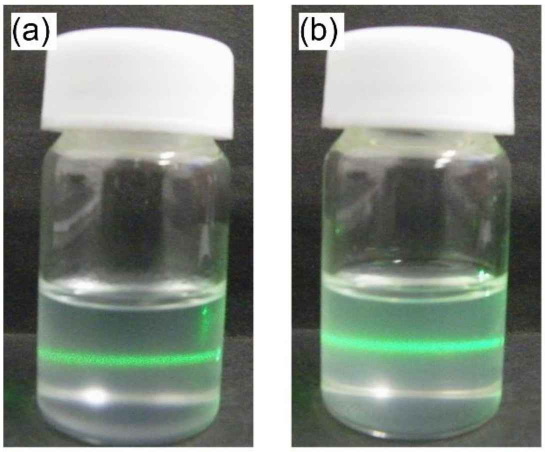

Fig. S3 Photographs of the as-synthesized solutions of (a) Mg-Tris-NH_2(90) and (b) Mg-Tris-NH_2(98).

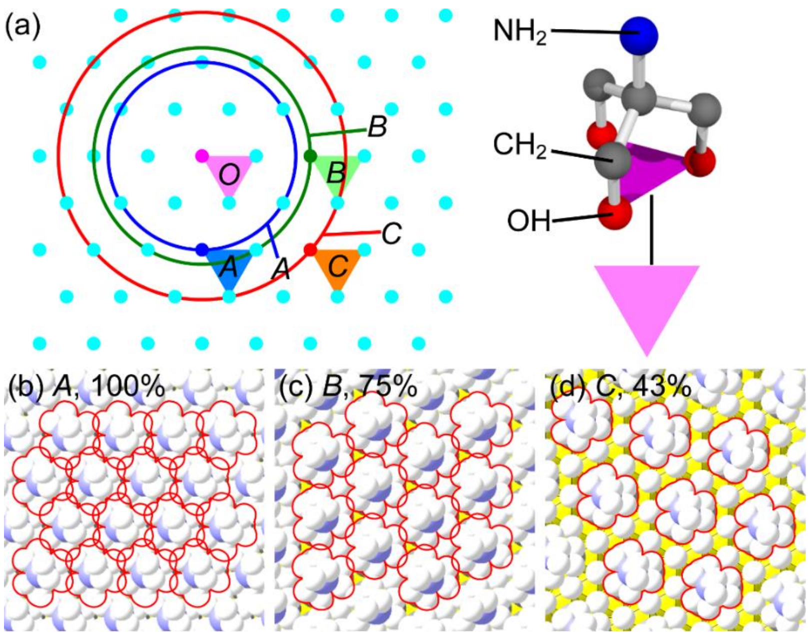

Fig. S4 (a) Schematic illustration of possible configurations of Tris-NH_2 immobilized through *tridentate* linkages on a brucite layer. Light blue dots represent the surface hydroxy groups in the a–b plane. A tripodal ligand is represented as a triangle whose corners correspond to the oxygen atoms. The triangle O (pink) represents the tripodal ligand at the origin. The triangles A (blue), B (green), and C (red) represent the first, second, and third neighboring positions to triangle O, respectively. (b–d) Structural models of the surface of Mg-Tris-NH_2 layers when Tris-NH_2 is placed according to the models (b) A (Tris-NH_2/Mg = 0.67), (c) B (Tris-NH_2/Mg = 0.50), and (d) C (Tris-NH_2/Mg = 0.29) shown in (a). Yellow octahedrons represent [MgO_6] units. White, gray, and blue spheres represent H, C, and N, respectively. A red circled area indicates a Tris-NH_2 molecule. Reprinted with permission from ref. 2 Copyright 2017 Wiley VCH.

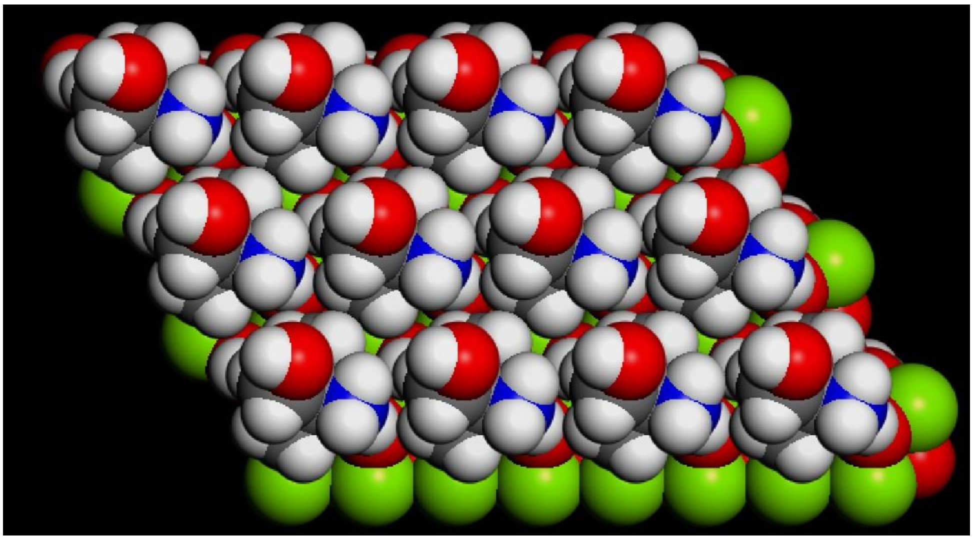

Fig. S5 Structural model of the surface of Mg-Tris-NH_2 layers when Tris-NH_2 is immobilized through *bidentate* linkages after the structural refinement by the DFT method. The arrangement of Tris-NH_2 in this model is the same as that of schematic illustration shown in Fig. S4c. The green, red, blue, gray, and white spheres represent Mg, O, N, C, and H, respectively. The sizes of the spheres represent the corresponding van der Waals diameters. The steric hindrance among the ligands is relaxed by structural flexibility due to some mobility of Tris-NH_2 with bidentate linkages.

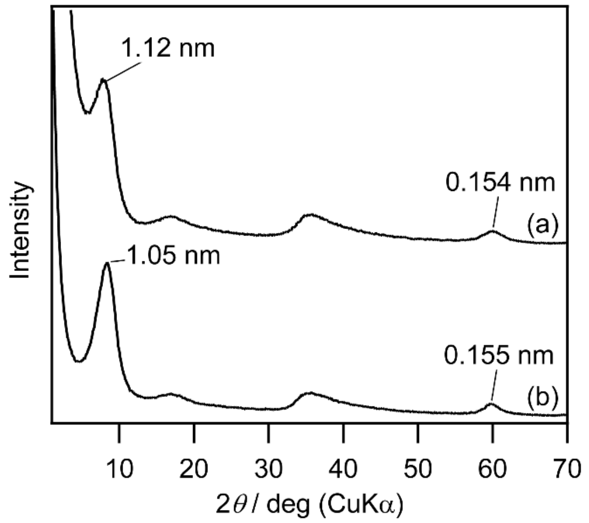

Fig. S6 XRD patterns of Mg-Tris-NH_2(98) (a) before and (b) after the water treatment.

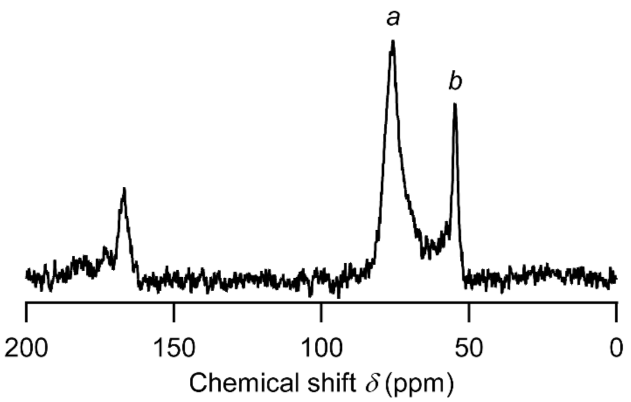

Fig. S7 ^{13}C CP/MAS NMR spectrum of Mg-Tris-NH_2(98) after the water treatment.

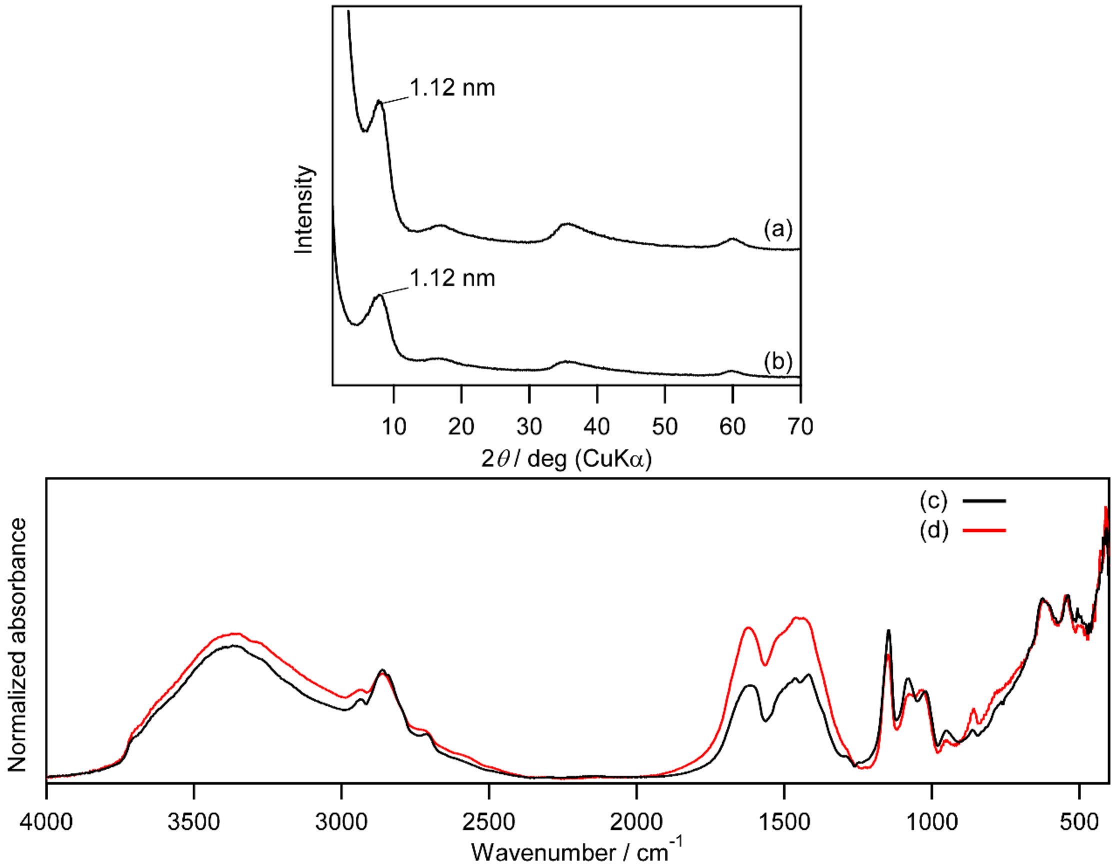

Fig. S8 (a, b) XRD patterns and (c, d) FTIR spectra of Mg-Tris-NH_2(98) measured (a), (c) just after synthesis and (b), (d) after storage in the atmosphere for about 22 months.

Interpretation of the FTIR spectra of Mg-Tris-NH_2(98) after long-term storage

In the FTIR spectrum, the absorbance of the characteristic bands due to both inorganic and organic species were mostly retained after the long-term storage (Fig. S8d), whereas some minor changes were observed in the ratio of absorbance in the region of 1000–1100 cm^{-1} (C–O stretching vibrations). The changes might reflect the hydrolysis of Mg–O–C bonds, though it is difficult to conclude it simply because various absorption bands such as C–O, C–C, and C–N stretching vibrations overlap in this region. The increase in the absorbance in 1400–1500 cm^{-1} is attributed to adsorption of CO_3^{2-}, which is usual for basic solids. Because the change in the infrared absorption is minor, we concluded that the hydrolysis due to atmospheric moisture is negligible or at least very slow.

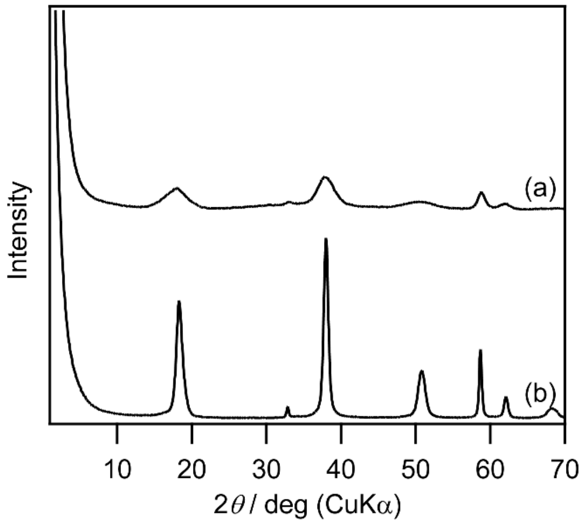

Fig. S9 XRD patterns of $Mg(OH)_2$ synthesized in (a) DMSO and (b) water by using TBAOH as a base.

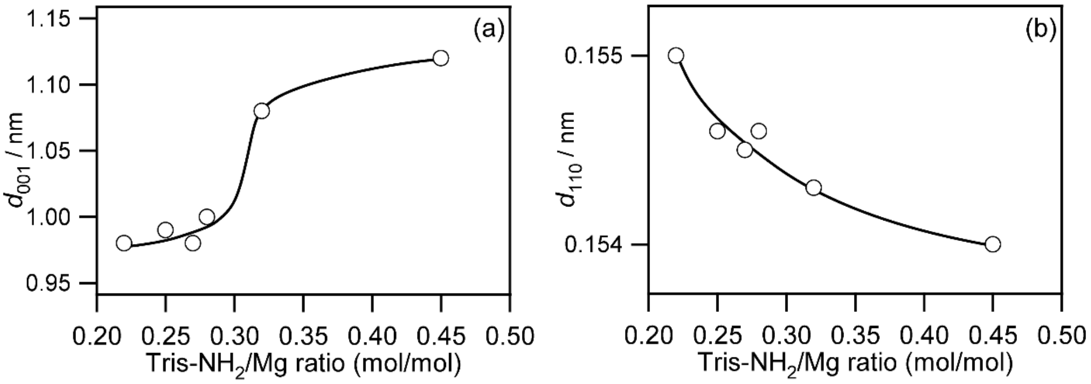

Fig. S10 Plots of (a) d_{001} and (b) d_{110} values versus Tris-NH$_2$/Mg ratios.

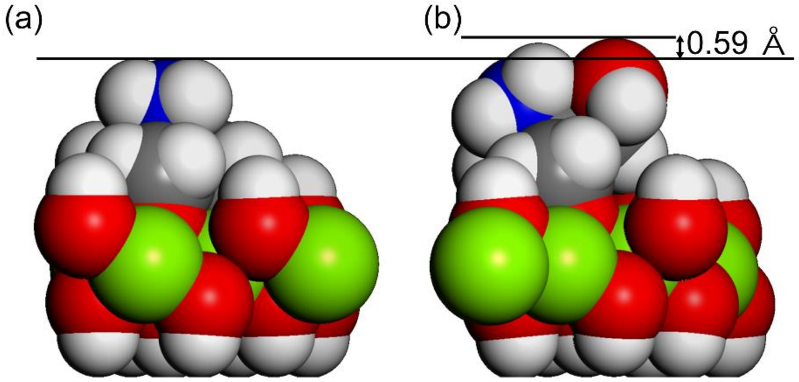

Fig. S11 Structural models of the brucite layers modified with Tris-NH$_2$ through (a) tridentate and (b) bidentate linkages after the structural refinement by the DFT method. The difference in the heights of Tris-NH$_2$ between these configurations was 0.59 Å; therefore, the difference in the d_{001} value will be between 0.59 Å (for the interdigitated structure) and 1.18 Å (for the bilayer structure). The green, red, blue, gray, and white spheres represent Mg, O, N, C, and H, respectively. The sizes of the spheres represent the corresponding van der Waals diameters.

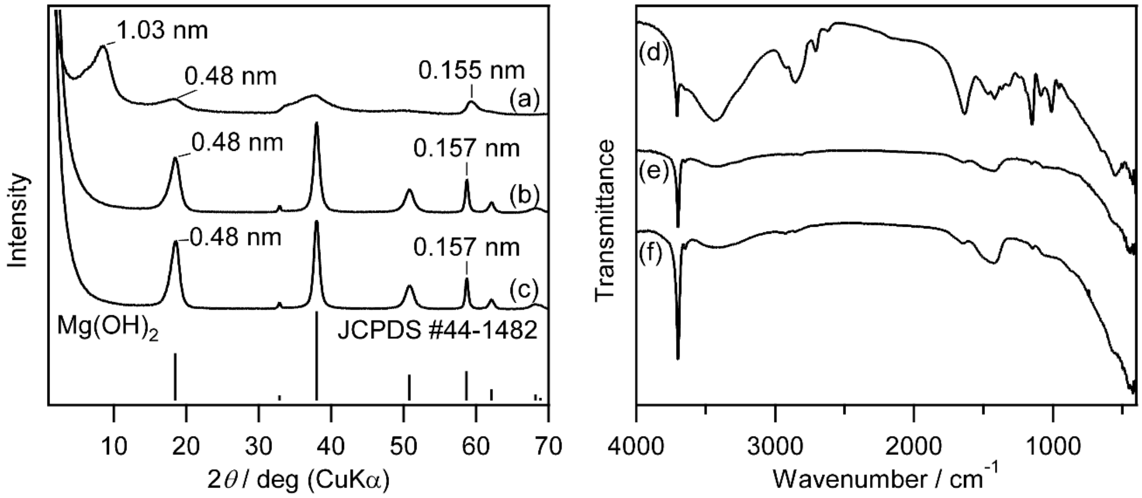

Fig. S12 (a–c) XRD patterns and (d–f) FTIR spectra of (a, d) Mg-Tris-CH_2OH, (b, e) Mg-Tris-CH_3, and (c, f) Mg-Tris-C_2H_5 synthesized in water.

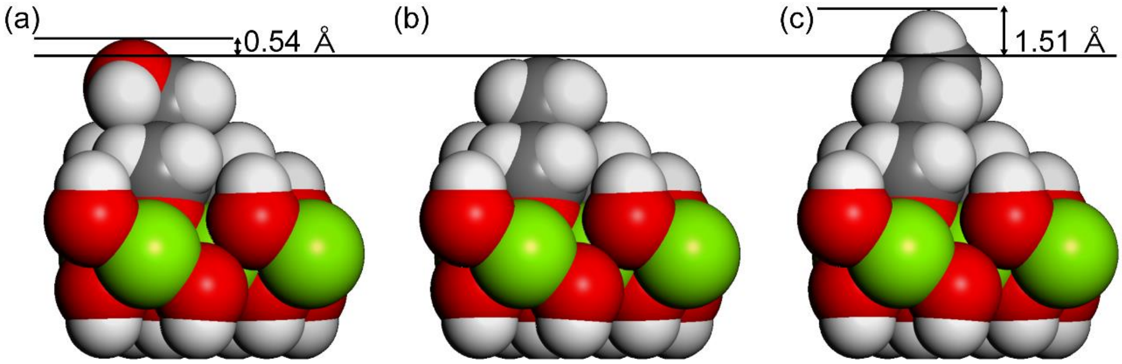

Fig. S13 Structural models of the brucite layers modified with (a) Tris-CH_2OH, (b) Tris-CH_3, and (c) Tris-CH_2CH_3 after the structural refinement by the DFT method. The green, red, gray, and white spheres represent Mg, O, C, and H, respectively. The sizes of the spheres represent the corresponding van der Waals diameters.

Table S2 Compositions of (a) Mg-Tris-CH_2OH, (b) Mg-Tris-CH_3, and (c) Mg-Tris-C_2H_5 synthesized in DMSO.

Sample	Mg (%)	C (%)	H (%)	N (%)	Cl (%)	Tris-*R*/Mg (mol/mol)	Yield (%)
Mg-Tris-CH_2OH	23.5	22.0	4.8	0.1	0.9	0.38	32
Mg-Tris-CH_3	26.8	18.6	4.3	0.0	0.5	0.28	31
Mg-Tris-C_2H_5	21.7	23.4	4.6	0.1	0.8	0.36	27

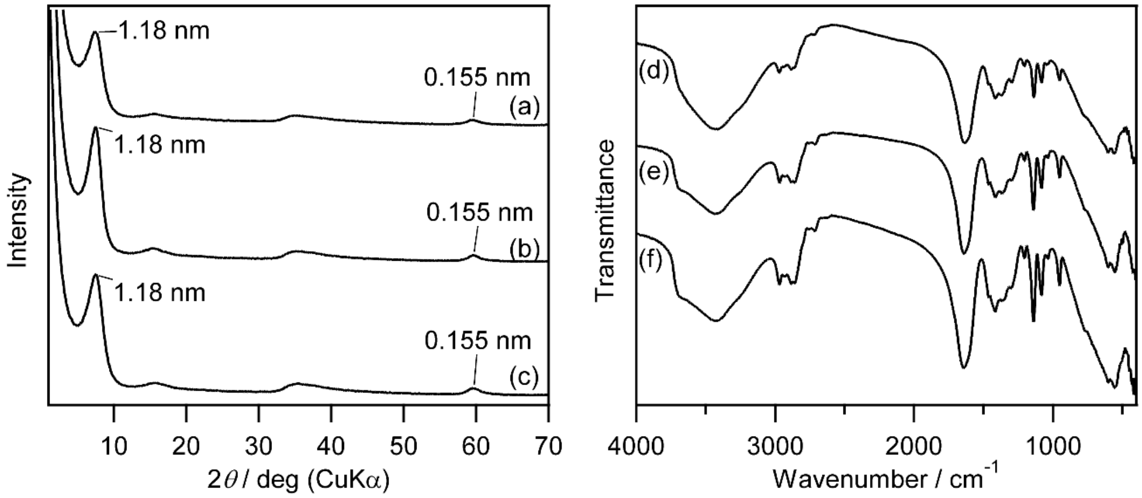

Fig. S14 (a–c) XRD patterns and (d–f) FTIR spectra of Mg-Tris-C_2H_5 synthesized in (a, d) DMSO, (b, e) DMF, and (c, f) DMA.

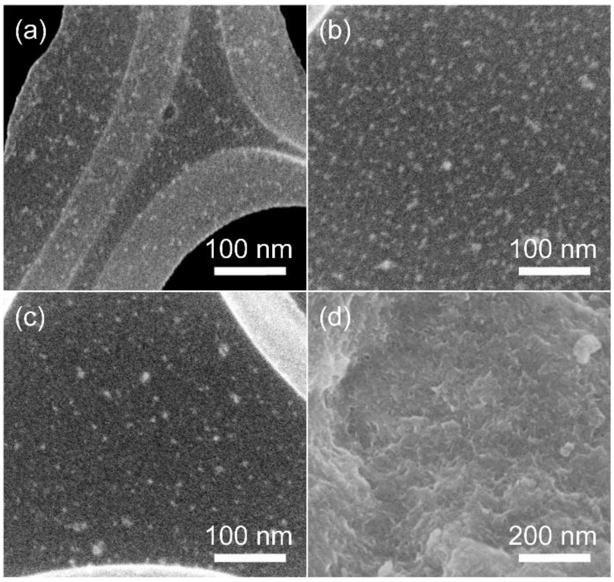

Fig. S15 SEM images of Mg-Tris-C_2H_5 synthesized in (a) DMSO, (b) DMF, and (c) DMA and (d) Mg-Tris-NH_2(98). The lateral size of primary particles is around 10 nm in all samples(a)–(c). Powdery samples were dispersed in ethanol and evaporated on a carbon-coated Cu grid for the observation. The image of (d) was obtained at an accelerating voltage of 3.0 kV.

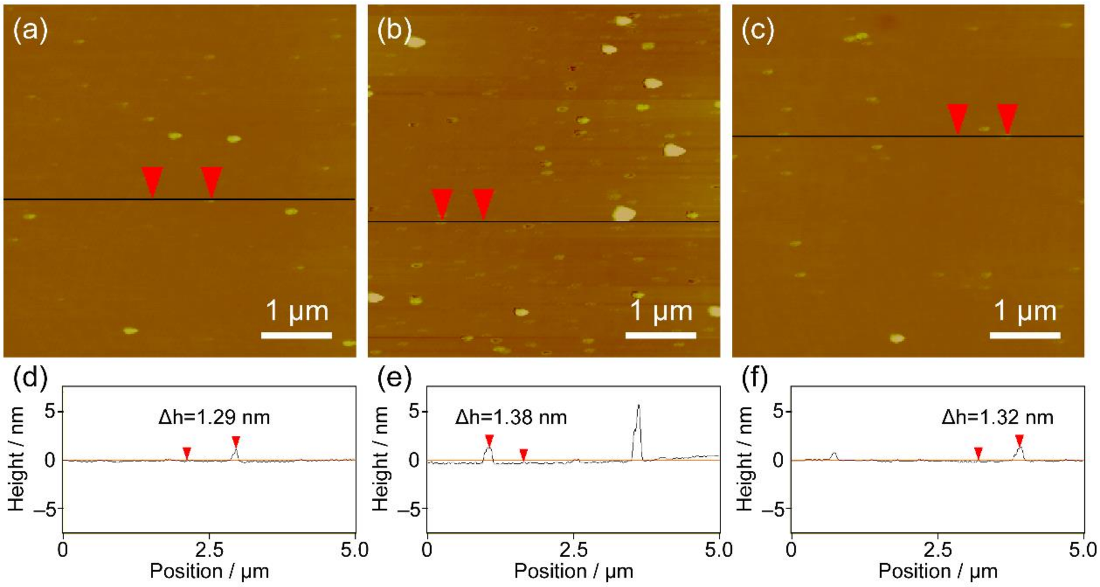

Fig. S16 (a–c) AFM images of Mg-Tris-C_2H_5 prepared by using (a) DMSO, (b) DMF, and (c) DMA as solvents. (d–f) The height profiles on the lines indicated in (a)–(c); (d) DMSO, (e) DMF, and (f) DMA.

References

1. S. Schroetter and D. Bougeard, *Ber. Bunsenges. Phys. Chem.* 1987, **91**, 1217–1221.
2. Y. Kuroda, T. Koichi, K. Muramatsu, K. Yamaguchi, N. Mizuno, A. Shimojima, H. Wada and K. Kuroda, *Chem. Eur. J.*, 2017, **23**, 5023–5032.